Available online at www.sciencedirect.com
ScienceDirect
Ceramics International 36 (2010) 521–527
CERAMICS INTERNATIONAL
www.elsevier.com/locate/ceramint

Influence of processing parameters on the electrical response of screen printed $SrFe_{0.6}Ti_{0.4}O_{3-\delta}$ thick films

A. Sanson [a,*], E. Mercadelli [a], E. Roncari [a], R. Licheri [b], R. Orrù [b], G. Cao [b], E. Merlone-Borla [c], D. Marzorati [c], A. Bonavita [d], G. Micali [d], G. Neri [d]

[a] *ISTEC-CNR, Via Granarolo 64, 48018 Faenza, RA, Italy*
[b] *Department of Chemical Engineering and Materials, University of Cagliari, DET-CNR, INSTM, Italy*
[c] *Centro Ricerche FIAT, Strada Torino, 50, 10043 Orbassano, TO, Italy*
[d] *Department of Industrial Chemistry and Materials Engineering, University of Messina, Italy*

Received 14 May 2009; received in revised form 19 July 2009; accepted 7 September 2009
Available online 12 October 2009

Abstract

A screen printing ink of $SrFe_{0.6}Ti_{0.4}O_{3-\delta}$ (STFO60) nanopowders produced by Self-propagating High-temperature Synthesis (SHS) was used to produce gas sensors with high level of reproducibility at low cost. The stability and rheology of the produced ink were studied in order to obtain high quality, highly reliable films. The electrical characteristics of the sensors as a function of the firing temperature and thickness of the sensing layer were investigated. The best results were obtained stabilizing the powder with lauric acid. Laboratory bench and on-road oxygen tests demonstrated that the response of 30 μm STFO60-based resistive sensors is comparable with the one of a commercial oxygen probe.

Keywords: $SrFe_{0.6}Ti_{0.4}O_{3-\delta}$; Oxygen sensors; Screen printing; Inks

1. Introduction

Modern combustion engines operate under lean conditions ($\lambda > 1$) [1]. To guarantee a precise engine control, fast and accurate oxygen sensors able to stand the aggressive conditions of the engine exhausts are needed. Iron doped strontium titanate ($SrFe_{0.6}Ti_{0.4}O_{3-\delta}$, STFO60) is a promising alternative to the commonly used zirconia for resistive oxygen sensors [2,3].

In order to meet the automotive industry's cost requirements, these sensors can be conveniently manufactured by screen printing. This is a simple and automated manufacturing technique that allows the production of low cost and robust chemical sensors with the required level of reproducibility leading to a general reduction of the sensors cost [4]. The technique is also compatible with the standard CMOS (Complementary Metal Oxide Semiconductor) processing and can be therefore applied for the production of fully integrated devices [5,6].

Several factors contribute to the success of producing high quality thick-film circuits, with the rheology of the thick-film paste being the most important one [7,8]. The ideal ink should have the proper degree of both pseudoplastic and thixotropic behaviour. The viscosity should remain low for a short time so that the printed film can level, filling the unevenness due to the screen wires. On the other hand, when the ink rests on the substrate, it is subjected to gravity and therefore to a very low shear rate. Under these conditions, its viscosity should quickly increase with time to prevent bleeding out of the film [9].

The key points to obtain a reliable and high performance sensors are the oxide intrinsic properties as well as an accurate manufacturing technique. Screen printing inks are complex non-equilibrium systems having flow properties strongly related to the nature and amount of their components [10]. Therefore a right blend of organic components is crucial to obtain a stable ink with suitable rheological properties.

The aim of this work was to study and optimize a screen printing ink of $SrFe_{0.6}Ti_{0.4}O_{3-\delta}$ nanopowders produced by Self-propagating High-temperature Synthesis (SHS) [11] to

* Corresponding author. Tel.: +0039 0546699 743; fax: +39 0546 46381.
E-mail addresses: alessandra.sanson@istec.cnr.it, sanson@istec.cnr.it (A. Sanson).

0272-8842/$36.00
doi:10.1016/j.ceramint.2009.09.028

allow the production of high performance low cost gas sensors with the right level of reproducibility. Sensors with different thermal treatments and thickness of the sensing layer have been investigated and their performance compared with those of a commercial electrochemical oxygen sensor.

2. Experimental

2.1. Powder synthesis and characterization

$SrFe_{0.6}Ti_{0.4}O_{2.8}$ (STFO60) powders were prepared by the Self-propagating High-temperature Synthesis (SHS) technique and subsequent ball-milling treatment (BM) as presented elsewhere [11]. They were characterized by B.E.T. single-point method (SSA) (Sorpy 1750, Carlo Erba, Italy), X-ray diffraction (Philips PW 1830, using Ni-filtered Cu Kα radiation, $\lambda = 1.5405$ Å) and scanning electron microscopy (SEM) (HITACHI S400, Japan).

2.2. Ink preparation and characterization

Terpineol-based inks were initially prepared in agate mortar and then transferred into a three-roller grinding mill equipped with zirconia rollers of nanometric finish (Exakt 80E, Exakt, Nordestedt, Germany) to improve homogeneity. Three deflocculants were tested for the dispersion of STFO60 powder in terpineol (Fluka, Germany): (1) a polyenoic ester (glycerol trioleate (GTO), Fluka, Germany); (2) a fatty acid (lauric acid (AL), Fluka, Germany) and (3) an heterocyclic acid (furoic acid (AF), Fluka, Germany). Ethyl cellulose (EC) (Fluka, Germany) was used as binder.

Rheological behaviour of the inks was analysed using a controlled-stress rotational rheometer (Bohlin C-VOR 120, Bohlin, Malvern, UK) equipped with serrated plates (diameter = 25 mm). Measurements were performed at 298 K by setting the plates distance at 500 μm. Viscosity-shear rate measurements were performed by sweeping over 22 values of shear rates (in logarithmic scale), the minimum and maximum being 0.01 and 100 s^{-1}, respectively. For each measurement a pre-shear of 2 min at 185 s^{-1} was first applied after which the shear rate was increased and then sequentially decreased.

Thixotropy has been investigated applying a rapid change of shear rate to the inks from a steady state at high shear rate to a lower one. The starting shear rate of 100 s^{-1} was chosen to simulate flow conditions through the meshes, while the values of lower shear rates (10, 1, 0.1 and 0.01 s^{-1}) mimic its evolution with time after the passage through the mesh. These jumps were applied following the sequential pattern according to the Camina–Roffey procedure.

Zeta potential measurements were performed on suspensions of the powder in terpineol (5 vol%) using an electroacoustic spectrometer (AcoustoSizer II, Colloidal Dynamics, Warwick, RI, USA). The instrument determines the ζ-potential of particles by fitting the dynamic mobility over a range of frequencies (from 1 to 18 MHz) of an imposed electric field. The same sound attenuation technique is used to measure the particle-size distribution necessary for the fitting.

2.3. Thick-film deposition

Thick films were screen printed (squeegee speed = 0.12 m/s, squeegee load = 6.5 kgF, snap off = 0.7 mm; AUR'EL 900, AUR'EL Automation S.p.A., Italy) onto alumina substrates (6 mm × 3 mm) supplied with comb-like electrodes and a Pt heater on the backside and left to dry at room temperature in air. A suitable mask was used to print each time the sensing element on a row of the ceramic substrate containing 12 interdigited structures.

The as-deposited films were analysed through optical microscopy (Leitz DMRME, Leica, Germany) and heat-treated at temperatures between 700 and 1100 °C. The sintered film microstructure was analysed using scanning electron microscopy and the film adhesion tested with the conventional scotch test.

2.4. Oxygen sensing tests

Sensing tests were performed at 650 °C with computer-assisted equipment running on LabView platform. The resistance measurements were done maintaining the sensors under a flow of dry nitrogen (200 cc/min) while pulsing different oxygen amounts in the range 0.1–20 vol%. Further details about the sensing tests procedure can be found elsewhere [11].

3. Results and discussion

3.1. Ink preparation

STFO60 nanopowders consist of agglomerates of about 5 μm (Fig. 1) with primary particle size of 40 nm, as calculated from XRD analysis. The specific surface area (SSA) corresponding to this particle dimension is 35.6 m^2/g [12]. The value is notably higher than the one obtained through nitrogen absorption (2.38 m^2/g). This effect is probably due to the agglomeration of the powder during the SHS process. The formulation of an ink with sub-micrometric powders is complicated by the large quantity of organics needed to ensure the desired rheology [13]. This high level of organics can easily lead to cracks during the heat treatment.

In order to obtain a stable and homogeneous ink, it is very important to effectively disperse the ceramic particles in the organic solvent (terpineol). The stability of the suspension depends on the effectiveness of the dispersant. The particles can be stabilized via one or a combination of two mechanisms: electrostatic repulsion or steric stabilization [14]. Among the three dispersant chosen, Glycerol Trioleate (GTO) is purely steric, furoic acid (AF) is purely electrostatic and lauric acid (AL) possesses a combination of electrostatic and steric activity. In order to find the most effective dispersant for the STFO60 system, sedimentation tests and zeta potential measurements were made. The sedimentation test can help to evaluate the efficiency of the dispersant with steric activity while the zeta potential analysis is used to test the performance of the electrostatic one. In the sedimentation test, the

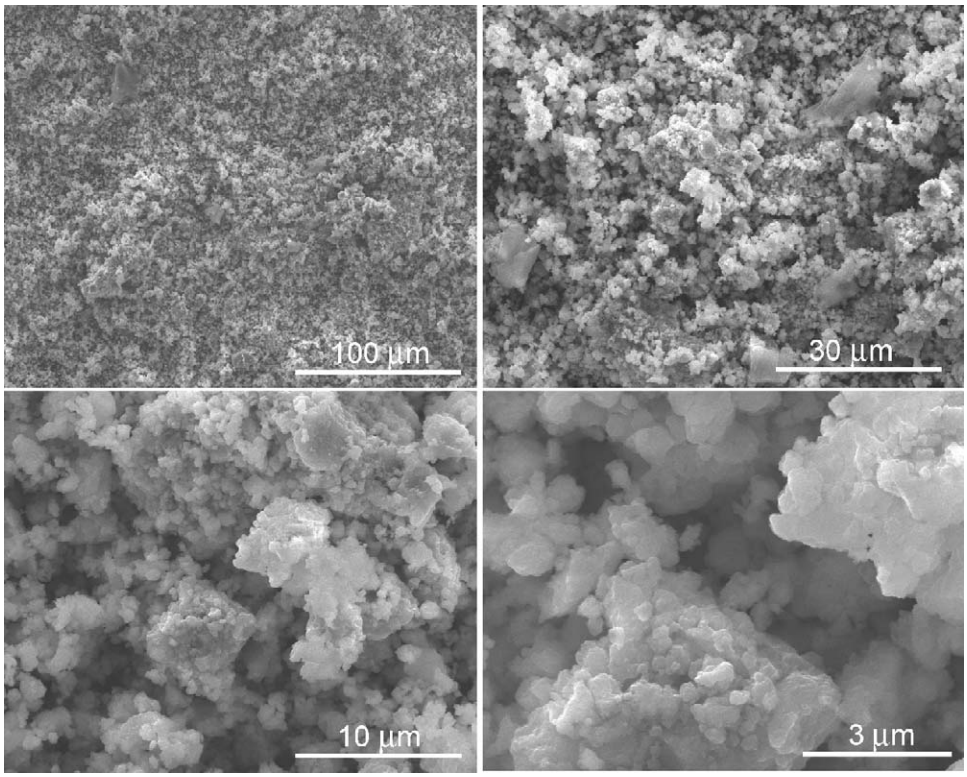

Fig. 1. SEM micrographs of the STFO60 powder obtained by SHS and BM (different magnifications).

suspensions of powder, solvent and dispersant were allowed to settle under gravity in air tight cylinders. Three different amounts of each dispersant (calculated as g dispersant for m^2 of powder) were considered: 1.5×10^{-3}, 2.0×10^{-3} and 2.5×10^{-3}. These values were chosen on the basis of previous analyses on screen printed inks of titanium-based oxides. The height of the sediment in each cylinder was measured as a percentage of the total solution height and used to define the most effective dispersant. The graph presented in Fig. 2 shows that the better stabilization is reached using AL in which the steric stabilization is accompanied by an electrostatic effect. In the case of GTO the stabilizing moiety is probably not very compatible with terpineol. As a consequence, the dispersant is not strongly solvated and the surface-coated particles of STFO60 tend to flocculate to minimize the tail–liquid interaction as already observed by Moloney et al. for zirconia suspension [14]. On the other hand, a pure electrostatic surfactant (AF) is not effective in stabilizing the system.

The stabilizing action of AL can be clearly seen from the trend of the ζ-potential reported in Fig. 3. Even if the measurements were quite noisy, due to the high viscosity of the medium, the influence of the two dispersants on the stability of the STFO60-terpineol suspensions can be analysed. The addition of AL caused a progressive increase in the values of ζ-potential (and consequently of the stability of the system) up to 2.2 ml where the potential reached a plateau centred at 100 mV, which is a typical value for a very stable suspension. The addition of AF led to a general decrease in stability

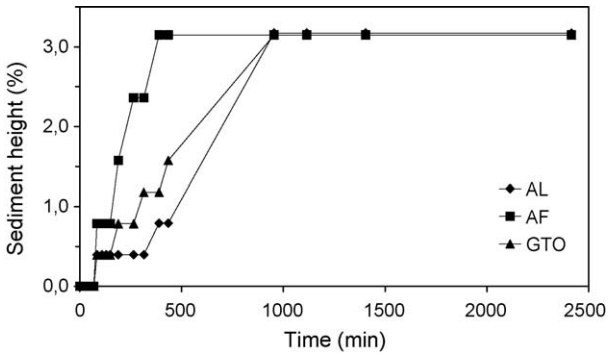

Fig. 2. Sedimentation tests of suspensions of STFO60 and 2×10^{-3} g dispersant/m^2 powder. Sediment height percentage relative to the initial height of the suspension. AF = furoic acid, AL = lauric acid, GTO = glycerol trioleate.

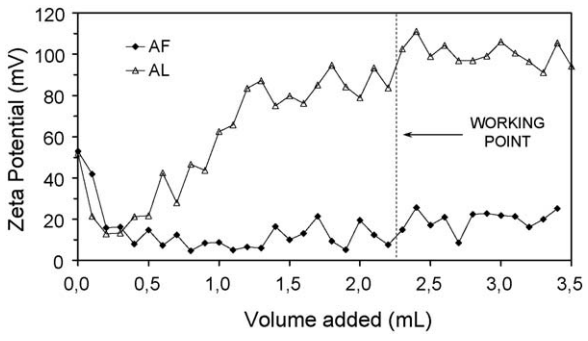

Fig. 3. ζ-potential of the STFO60 suspensions titrated with solutions of AF and AL.

responsible of the sedimentation observable also from the curves of Fig. 2. GTO is not considered because its action is purely steric and then not detectable with this technique.

3.2. Film deposition

The ink formulations described above were used to print STFO60 thick films on interdigited ceramic substrates. To check the influence of dispersion on the printed film, two inks (indicated as AF and AL1) were made using AF and AL, their compositions are reported in Table 1. A poor stabilization of the powder caused bleed-out of the ink as a consequence of the

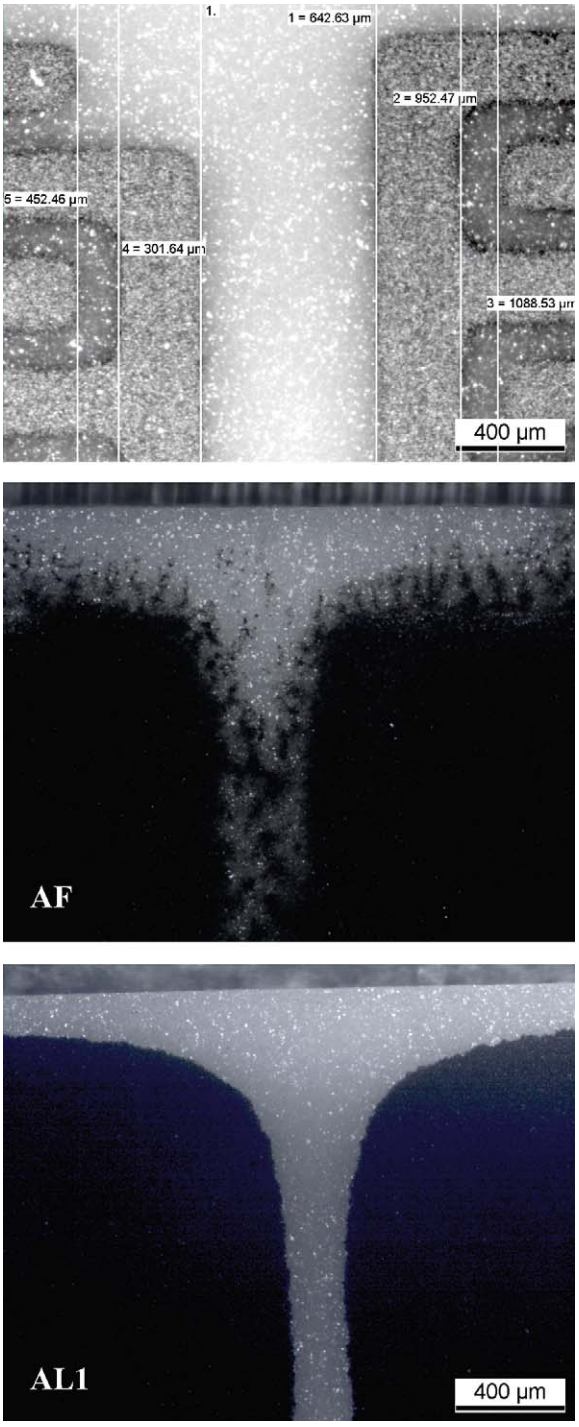

Fig. 4. Optical micrographs of the green layers obtained with an AF ink or AL1 ink. On the top is presented a detail of the Pt interdigits on which the sensing layers are deposited.

Table 1
Composition (wt%) of the inks made.

Ink code	STFO60	Terpineol	Furoic acid	Lauric acid	Ethyl cellulose
AF	41.68	50.18	0.03	–	2.11
AL1	41.68	50.18	–	0.03	2.11
AL2	61.47	35.38	–	0.04	3.11

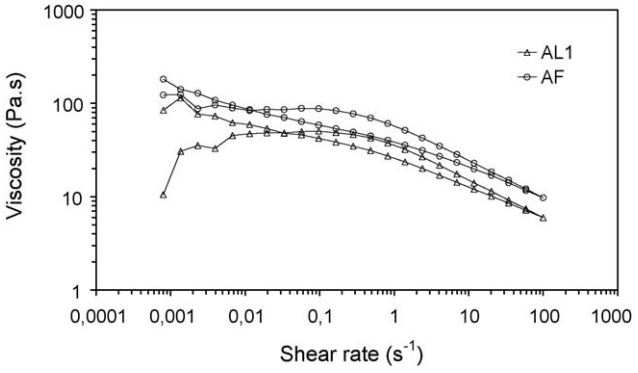

Fig. 5. Flow curves of the inks made using AF and AL1 as dispersant.

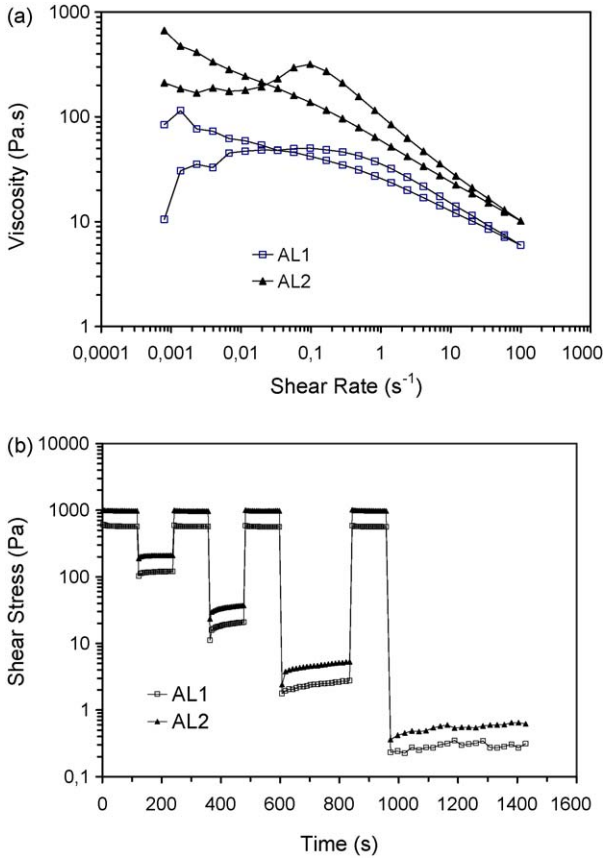

Fig. 6. Flow curves (a) and thixotropic behaviour (b) of the two inks made with lauric acid as dispersant.

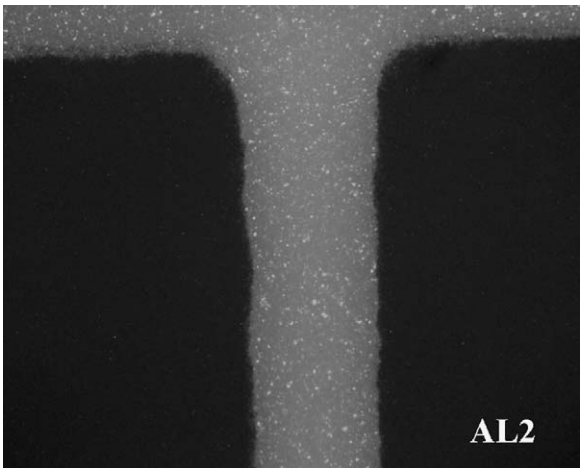

Fig. 7. Green layers of STFO60 obtained depositing the AL2 ink.

organics released from the printed slurry at the pattern edges that dragged along some debris (Fig. 4). The layer obtained with the AL ink, even if not affected by bleed-out, did not show the required resolution for sensor applications probably as a consequence of the low values of viscosity.

In Fig. 5 the flow curves of AF and AL1 are presented. Both the systems show values of viscosity lower than the ones generally accepted for screen printing inks [9]. Moreover, AL1 led to lower values of viscosity with respect to AF as a consequence of its better dispersion ability. Two different strategies can be applied to reach higher values of viscosity and consequently higher resolution: (i) reduce the amount of solvent and (ii) increase the amount of binder. The second one leads to a more complicated burn-out cycle and it is generally avoided. A second lauric-based ink was then formulated keeping constant the powder/binder and $g_{dispersant}/m^2_{powder}$ ratios and lowering the percentage of solvent (AL2, Table 1). The effect of this reduction on the flow curve and thixotropic behaviour of the ink is presented in Fig. 6. This second ink showed values of viscosity well inside the range suitable for the screen printing process (a) and a more structured polymer network as indicated by the higher degree of thixotropy (b). This improved rheology led to a remarkable increase in print definition as shown by the optical micrographs of Fig. 7.

The films obtained with the AL2 ink were then heat-treated at 700, 850 and 1100 °C with dwelling time of 30 min to remove the organics and stabilize the microstructure.

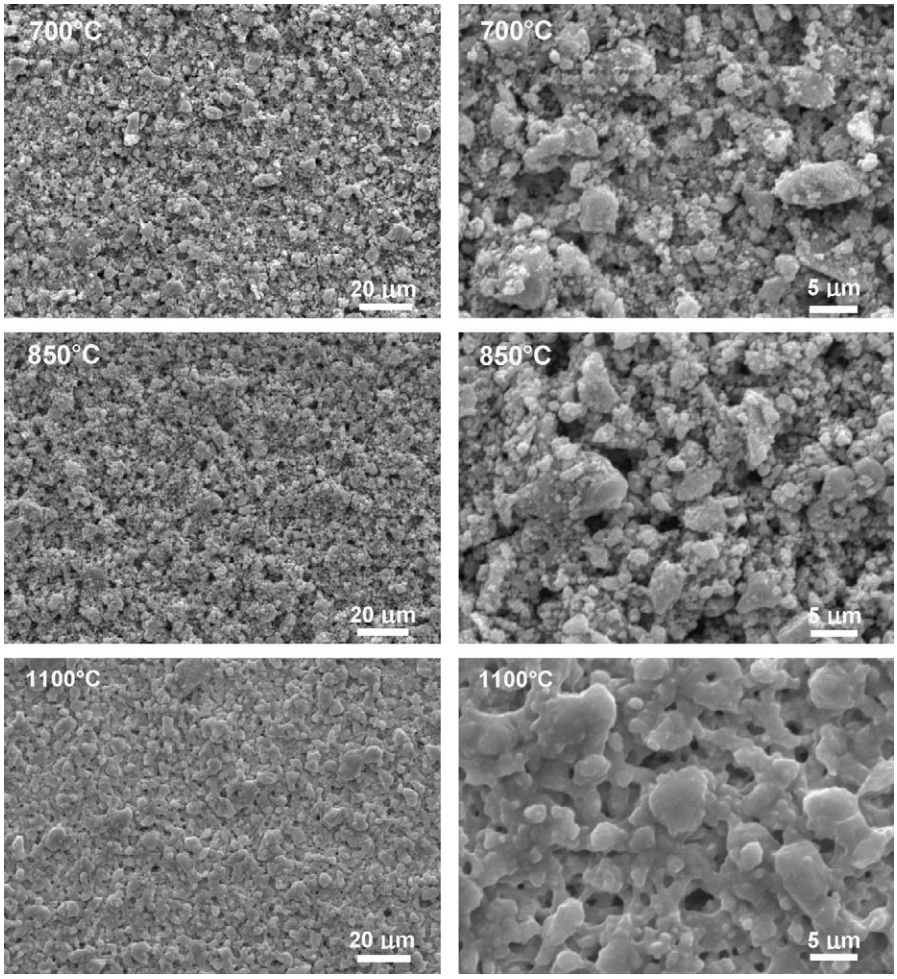

Fig. 8. SEM micrographs of the films sintered at 700, 850 and 1100 °C for 30 min.

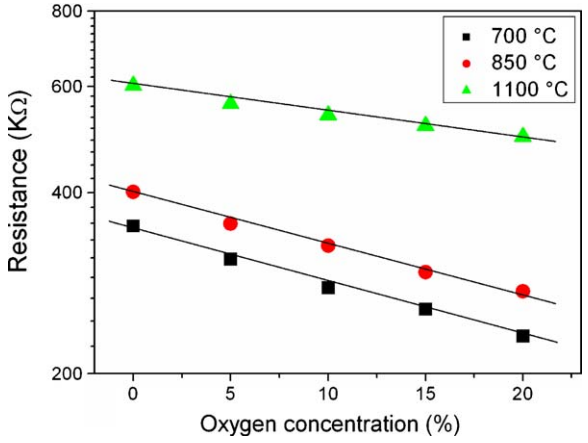

Fig. 9. Resistance vs. oxygen concentration for the STFO60 film sintered at 700, 850 and 1100 °C.

The temperatures reached by the exhaust gas of a diesel engine downstream from the turbocharger are in the range of 800–850 °C at full load; for this reason, the sensors microstructure has to be stable up to such temperatures in order to maintain good film sensing properties.

The microstructures of the layers treated at the above mentioned temperatures are reported in Fig. 8. As expected, at 1100 °C the film showed a high degree of sintering, although only a small increase in particle size was detectable. On the other hand the treatment at 850 °C gave results not significantly different from those obtained at 650 °C. In addition, the scratch-tests done on the sintered films revealed an higher adhesion for the former, indicating its better mechanical stability. It is worth noticing, that the formulation of the inks was capable of preventing crack formation during the heat treatment.

3.3. Oxygen sensing tests

Preliminary measurements have been carried out to investigate the effect of the thermal treatment and film thickness on the electrical and sensing characteristics of the screen printed layer. The firing temperatures chosen were the same as those previously considered for the sintering experiments. Previous experiments carried out on the STFO60 sensor have shown an increase of the baseline resistance (i.e. at 0% oxygen concentration) with an increasing of the firing temperature (Fig. 9). The same trend was observed at all oxygen concentration tested. This latter behaviour can be related to the massive sintering of the sensitive grains with the reduction of surface area occurring at the highest temperature tested, as shown by the SEM picture of Fig. 8. Moreover, as STFO60 behave as a p-type semiconductor in the region of oxygen concentration tested, a decrease of surface oxygen coverage due to surface area loss increases consequently the resistance, as experimentally observed. Although the study of the sensing mechanism on the STFO sensors is out of the scope of the present paper, the higher response observed on the more porous films (i.e. those fired at lower temperature) seems to indicate that a surface controlled mechanism is operative, and consequently the accessible surface area is the most important parameter in controlling the sensor response. On the other hand, the operating temperature of the sensor (650 °C) is at borderline between a surface- and bulk-controlled mechanism and a more detailed investigation is necessary to better understand the true oxygen sensing mechanism of these materials in the experimental conditions adopted.

On the basis of these results it was decided to investigate the sensing properties of the STFO60 film after firing at 700 °C. Films were deposited on alumina substrates and tested to determine the response to a variation of thickness (Fig. 10) and oxygen concentration (Fig. 11). Measures were carried out in nitrogen flow and after equilibration the sensors were exposed to different oxygen concentrations in nitrogen carrier until signal saturation.

The resistance baseline of the thinner sensor is higher than that of the thicker one. Moreover, while the resistance baseline of the former is not stable during pulses at different oxygen concentrations showing a continuous drift towards higher resistance values, the 30 μm-thick sensor is more stable (Fig. 10a) even considering longer time (Fig. 10b). Initially the response of the two sensors is the same, but the response of the thinner film decreases with time. This behaviour could be explained by considering a depletion of Fe at or near the film–

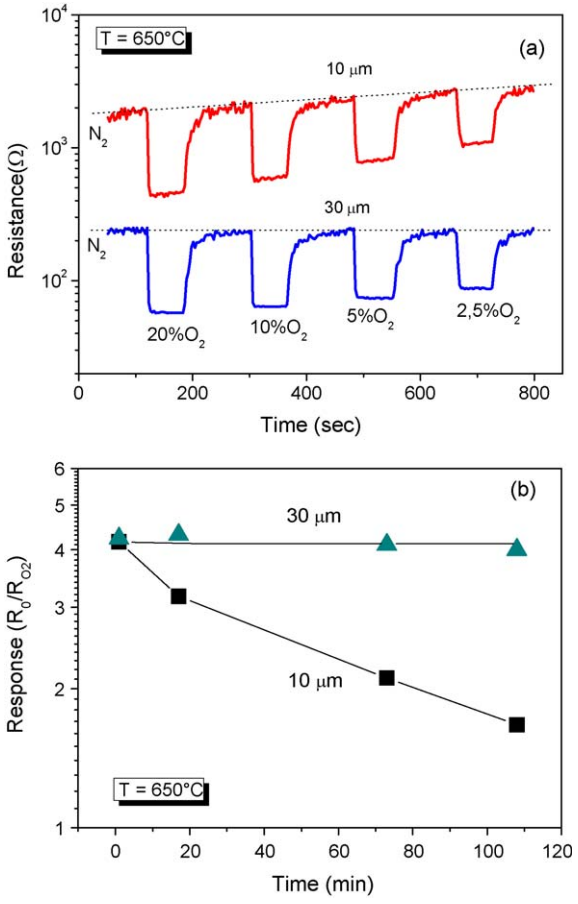

Fig. 10. (a) Transient response of STFO60 sensors with different sensing layer thicknesses and (b) response of the sensors to repeated 20% oxygen pulses. R_0 is the resistance in N_2 and R_{O_2} that in 20% O_2.

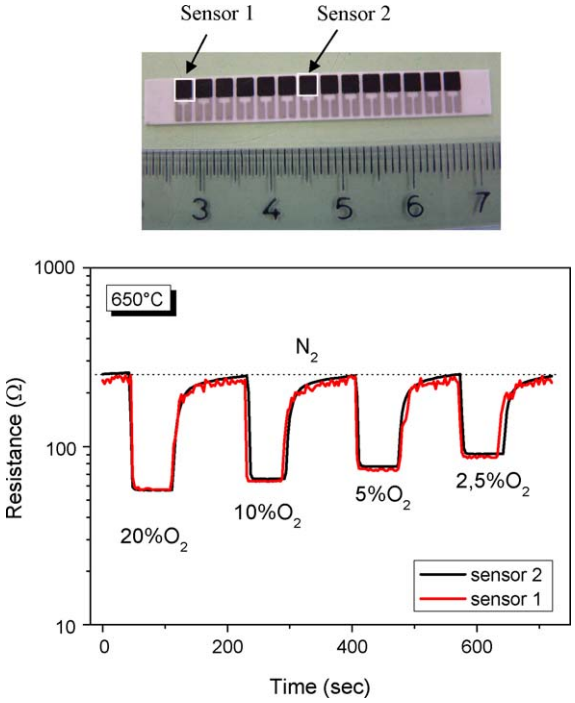

Fig. 11. Bench tests on two different sensors (see photo on the top) showing the reproducibility of the response.

substrate interface, as suggested by Litzelman et al. for STFO films on sapphire [15]. A dedicated study is however necessary to better understand this effect.

To test the reliability of the screen printing process, the response of two sensors prepared printing the STFO60 film in a single operation on a row of the ceramic substrate containing 12 interdigited structures was compared. Fig. 11 reports the transient response registered at 650 °C at different oxygen concentrations with total flow of 200 cc/min. The sensing characteristics of the sensors (baseline resistance, response and response/recovery times) are almost coincident confirming that

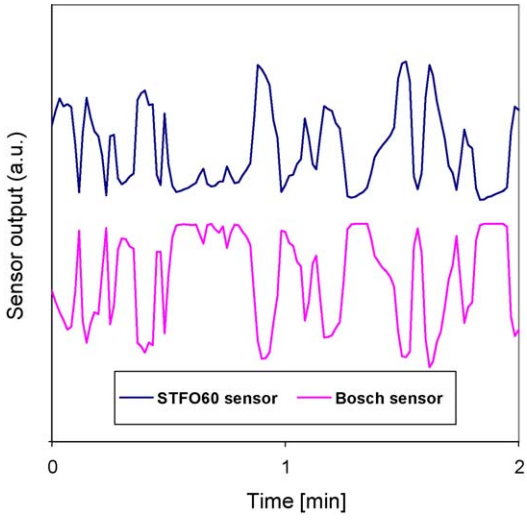

Fig. 12. Comparison of the output of the STFO60 sensor with the one of the Bosch UHEGO probe during a road test.

the optimization of the ink formulation produces a high level of reproducibility of the electrical and sensing characteristics of the layers deposited.

Following these encouraging results the performances of the STFO sensor were tested in real conditions on a diesel car. In Fig. 12 the comparison between the sensor response of the STFO60 sensor and that of a commercial electrochemical sensor (UHEGO, Bosch) is presented. The good correspondence in terms of sensitivity and response time indicates that the resistive STFO60 sensor shows performance comparable with those of the commercial electrochemical oxygen probe. A more complete analysis of the data collected during these tests is reported in detail elsewhere [16].

4. Conclusions

Screen printed $SrFe_{0.6}Ti_{0.4}O_{3-\delta}$ films were deposited on an alumina interdigitated substrate for the production of resistive oxygen sensors. The use of $SrFe_{0.6}Ti_{0.4}O_{3-\delta}$ nanopowders produced by SHS induces a high response of the sensing layer but introduces additional constrains on the ink formulation for the screen printing process. A deep study on the dispersion behaviour of the powder and on the rheology of the ink was mandatory to obtain high quality, high reliable films with performances comparable with the one of the UHEGO oxygen sensor commercialized by Bosch.

Acknowledgments

The authors gratefully acknowledge the financial support of MUR under the FIRB-SqUARE project (contract number RBNE01Y8C3). Dr. Gardini is acknowledged for the ζ-potential measurements.

References

[1] R. Moos, F. Rettig, A. Hurland, C. Plog, Sens. Actuators B 93 (2003) 43–50.
[2] R. Moos, PhD thesis, Karlsruhe, VDI-Verlag, Dusseldorf, 1994.
[3] R. Moos, W. Menesklou, H.-J. Schreiner, K.H. Hardtl, Sens. Actuators B 67 (2000) 178–183.
[4] G. Martinelli, M.C. Carotta, Sens. Actuators B 23 (1995) 157–161.
[5] N.M. White, J.D. Turner, Meas. Sci. Technol. 8 (1997) 1–20.
[6] F. Menil, H. Debeda, C. Lucat, J. Eur. Ceram. Soc. 25 (2005) 2105–2113.
[7] M.R. Parikh, W.F. Quilty, K.M. Gardiner, IEEE Trans. Comp. Hybrids Manuf. Technol. 14 (3) (1991) 493–498.
[8] J. Savage, Thin Solid Films 4 (1969) 137–148.
[9] R.E. Trease, R.L. Dietz, Solid State Technol. (1972) 38–43.
[10] R.W. Vest, Ceram. Bull. 65 (4) (1986) 631–636.
[11] G. Neri, A. Bonavita, G. Micali, G. Rizzo, R. Licheri, R. Orrù, G. Cao, Sens. Actuators B 126 (2007) 258–265.
[12] P.A. Webb, C. Orr, Micromeritcs, 1st ed., 1997.
[13] M.C. Carotta, M. Ferroni, V. Guidi, G. Martinelli, Adv. Mater. 11 (11) (1999) 943–946.
[14] V.M.B. Moloney, D. Parris, M.J. Edirisinghe, J. Am. Ceram. Soc. 78 (12) (1995) 3225–3232.
[15] S.J. Litzelman, A. Rothschild, H.L. Tuller, Sens. Actuators B 108 (2005) 231–237.
[16] G. Neri, G. Micali, A. Bonavita, R. Licheri, R. Orrù, G. Cao, D. Marzorati, E. Merlone Borla, E. Roncari, A. Sanson, Sens. Actuators B 134 (2) (2008) 647–653.